Computer Physics Communications 32 (1984) 239–243
North-Holland, Amsterdam

NEW EFFICIENT ALGORITHM FOR SOLUTION OF THE DRIVEN NONLINEAR SCHRÖDINGER EQUATION

Milivoj R. BELIĆ, Slobodan VUKOVIĆ
Institute of Physics, P.O.Box 57, 11001 Beograd, Yugoslavia

and
Melvin LAX *
Physics Department, City College of the City University of New York, New York, NY 10031, and Bell Laboratories, Murray Hill, NJ 07974, USA

Received 20 December 1983; in revised form 7 February 1984

An efficient and reliable numerical algorithm for solution of the driven nonlinear Schrödinger equation:
$i\partial_t A(x, y, t) + \Delta A - (x - p|A|^2)A = \hat{x}$
and Zakharov's equations in 2+1 dimension is presented. The algorithm is an FFT-based modified thin-sheet correction scheme.

1. Introduction

The driven nonlinear Schrödinger equation (DNLSE) describes resonant absorption of electromagnetic waves and generation of density cavities in an inhomogeneous plasma when the effect of ion inertia is neglected [1–3]. Formation of the cavities is accompanied by the development of a transient solitary wave structure in the electromagnetic field ("soliton flash" [4]). In view of the problems concerning the stability of stationary solutions in 1 + 1 dimension (one space, one time) [3–6], as well as the collapse of Langmuir solitons in 2 + 1 dimensions [2,7], we present an alternative reliable and efficient method for numerical solution of DNLSE. The method is also applied to the case when ion inertia is taken into account, and a strong Landau or collisional damping of ion waves assumed. This case is described by a coupled set of differential equations (Zakharovś equations) for the electric field and plasma density [2–7].

The algorithms thus far used in numerical treatment of DNLSE include the time-averaged Crank–Nicholson procedure [3], Numerov scheme in space, with a leapfrog in time [6], and a method of spectral representation of the derivatives, with nonlinearities computed via Fourier transform to configuration space [7]. Other spectral algorithms are used as well [8], but they bear little resemblance to the method described in this paper.

While in spirit similar to that of ref. [7], our method contains many new features which render it useful and worthwhile for presentation to the computer oriented physics community. The method represents a modification of the thin-sheet gain procedure [9–11] developed earlier for the mode calculation in a high-power laser.

2. Numerical procedure

The driven nonlinear Schrödinger equation for a two-component scaled electric field $A = (A_x, A_y)$ is of the form [3,6]:

$$i\partial_t A_x(\boldsymbol{\rho}, t) + \Delta A_x - mA_x = 1, \qquad (2.1a)$$

$$i\partial_t A_y(\boldsymbol{\rho}, t) + \Delta A_y - mA_y = 0, \qquad (2.1b)$$

* Supported in Part by the Army Research Office.

where $m = x - p(|A_x|^2 + |A_y|^2)$ represents the nonlinear medium interaction term (p is the nonlinearity coefficient), $\Delta \equiv \partial_x^2 + \partial_y^2$ represents the two-dimensional Laplacian, and $\boldsymbol{\rho} = (x, y)$. Except for the detailed structure of m, eq. (2.1b) is in form analogous to the paraxial wave equation, which has been treated by the thin-sheet gain procedure elsewhere [10,11], and therefore will not be analysed here. However, the essential ingredients of the thin-sheet gain or correction procedure, as well as modifications needed in treatment of eq. (2.1a) will be given here.

Indeed, if in eq. (2.1a) m were zero, the remaining equation is linear, and thus easily solved by the Fourier transform technique. In that case we take two-dimensional spatial Fourier transform of eq. (2.1a) (subscript x is omitted):

$$\mathrm{i}\partial_t \bar{A}(\boldsymbol{q}, t) - q^2 \bar{A} = \delta(\boldsymbol{q}), \tag{2.2}$$

where

$$\bar{A}(\boldsymbol{q}, t) = \int \frac{\mathrm{d}^2\rho}{(2\pi)^2}\, \mathrm{e}^{-\mathrm{i}\boldsymbol{\rho}\cdot\boldsymbol{q}} A(\boldsymbol{\rho}, t) \tag{2.3}$$

is the direct Fourier transform, and $\delta(\boldsymbol{q})$ is the two-dimensional delta function. Then:

$$\bar{A}(\boldsymbol{q}, t) = \mathrm{e}^{-\mathrm{i}q^2 t}\bar{A}(\boldsymbol{q}, 0) + \frac{\mathrm{e}^{-\mathrm{i}q^2 t} - 1}{q^2}\delta(\boldsymbol{q}), \tag{2.4}$$

or in the configuration space:

$$A(\boldsymbol{\rho}, t) = (\mathrm{FT})^{-1}\, \mathrm{e}^{-\mathrm{i}q^2 t}(\mathrm{FT}) A(\boldsymbol{\rho}, 0) - \mathrm{i}t, \tag{2.5}$$

where (FT) $[(\mathrm{FT})^{-1}]$ denotes the direct [inverse] Fourier transform. Therefore, a formal solution of eq. (2.1a) with $m = 0$,

$$A(\boldsymbol{\rho}, t) = \mathrm{e}^{\mathrm{i}t\Delta} A(\boldsymbol{\rho}, 0) - \mathrm{i}t \tag{2.6}$$

actually corresponds to a sequence of operations described by eq. (2.5). An equally formal solution of the full eq. (2.1a):

$$A(\boldsymbol{\rho}, t) = \mathrm{e}^{\mathrm{i}F}\left[A(\boldsymbol{\rho}, 0) - \mathrm{i}\int_0^t \mathrm{e}^{-\mathrm{i}F}\right], \tag{2.7}$$

with $F = t\Delta - \int_0^t m = t(\Delta - \langle m \rangle)$, can also be broken into a sequence of operations to be performed upon the initial field $A(\boldsymbol{\rho}, 0)$. We preferred a simple sequence correct up to the third order in time step h [10]:

$$A(\boldsymbol{\rho}, t_{n+1}) = \mathrm{e}^{\mathrm{i}h\Delta/2}\, \mathrm{e}^{-\mathrm{i}h\langle m \rangle}\, \mathrm{e}^{\mathrm{i}h\Delta/2} A(\boldsymbol{\rho}, t_n) - \mathrm{i}h - h^2\langle m \rangle/2. \tag{2.8}$$

The first operator to act on $A(\boldsymbol{\rho}, t_n)$ is the same as in eq. (2.6) or (2.5), only here it acts over the interval $h/2$ – it is therefore a free-space propagator for $h/2$. The medium correction terms $\exp(-\mathrm{i}h\langle m \rangle)$ and $-h^2\langle m \rangle/2$ require evaluation of the mean of m across the (presumably small) time step. While a more elaborate procedure might be thought of, we simply use m evaluated at the current value of t for $\langle m \rangle$. In this manner we save computer core space and make simple and efficient code. In this approach the continuous temporal development is approximated by a series of medium (or vertex) corrections in-between which the temporal advance is achieved by the free-space propagation. This is referred to as the thin-sheet correction approximation [9–11].

The error and stability analysis of the thin-sheet procedure have previously been performed in the context of beam propagation in the atmosphere [10] and in a lasing medium [11]. Here we only outline the crucial steps in this analysis without being too rigorous. Looking at eq. (2.7) it is seen that operator F, which figures in the exponent, actually presents a sum of two noncommuting operators $h\Delta$ and $h\langle m \rangle$. Therefore adequate care must be paid to the ordering of these operators as we advance in time. By writing $\exp(\mathrm{i}F)$ as $\exp(\mathrm{i}h\Delta/2)\exp(C)\exp(\mathrm{i}h\Delta/2)$ and by utilizing the Baker–Hausdorff theorem it is seen that C equals $-\mathrm{i}h\langle m \rangle$ if double and higher order commutators of $h\Delta$ and $h\langle m \rangle$ are neglected, and if $\langle m \rangle$ does not vary appreciably with h. In this case eq. (2.8) results, and the procedure is of the third order in h. Among the neglected terms the most troublesome for stability analysis are of the order h^3/δ^4, where δ is the size of the spatial increment (which is proportional to the inverse of the spectral resolution in the reciprocal space). This estimate appears favourable when compared to the usual h/δ^2 value found in difference methods for this type of parabolic equations. An additional error is introduced by using m evaluated at the current value of t for $\langle m \rangle$. Here, however, the accuracy can be improved (for example by devising a self-consistent iteration procedure [11]) at the expense of computer time and memory requirements.

The overall one-step procedure for both field components A_x, A_y is given by:

$$A_x(\rho, t_{n+1}) = (\mathrm{MPR}) A_x(\rho, t_n) - \mathrm{i}h - h^2 m_n/2, \qquad (2.9\mathrm{a})$$

$$A_y(\rho, t_{n+1}) = (\mathrm{MPR}) A_y(\rho, t_n), \qquad (2.9\mathrm{b})$$

where

$$(\mathrm{MPR}) \equiv \mathrm{e}^{\mathrm{i}h\Delta/2}\, \mathrm{e}^{-\mathrm{i}hm_n}\, \mathrm{e}^{\mathrm{i}h\Delta/2} \qquad (2.10)$$

represents the medium propagator.

The complete sequence of operations then looks as follows. Starting from some suitably chosen initial field $A(\rho, 0)$, this field is free-propagated for an interval $h/2$ to the first correction sheet, where medium correction (over the whole interval h) is performed; the resulting field is propagated for another $h/2$, and at the end the inhomogeneous part $-\mathrm{i}h - h^2 m_n/2$ is added to the x-component. This completes one step in time. The procedure is then repeated for as many h steps, or as many correction sheets as needed.

This relatively simple code is easy to implement. For calculation of the Fourier transform we use an FFT algorithm. In order to prevent reflection from the grid edges and spillover effects [11], the field is damped close to the edges. To avoid occurrence of the saw-tooth instabilities, after certain number of time steps a data-smoothing is performed.

The code equally well applies to the more complete case when ion inertia is taken into account, and a strong Landau damping of ion waves assumed. This case is described by a coupled set of equations for the electric field and plasma density [2–7]:

$$\mathrm{i}\partial_t A + \Delta A - (x + pN) A = \hat{x}, \qquad (2.11\mathrm{a})$$

$$\gamma \partial t_N - \Delta N = \Delta |A|^2, \qquad (2.11\mathrm{b})$$

where γ is the damping factor. While the analysis of eq. (2.11a) proceeds as before, numerical treatment of eq. (2.11b) requires some modifications. In order to make a simple code we used the following scheme:

$$N_{n+1} = (\mathrm{FT})^{-1}(\exp)(\mathrm{FT}) N_n + (\mathrm{FT})^{-1} \times [(\exp) - 1](\mathrm{FT}) |A_n|^2, \qquad (2.12)$$

where N_n denotes $N(\rho, t_n)$ and (exp) denotes $\exp(-q^2 h/\gamma)$. This scheme, as is obvious from our results, suites our qualitative analysis perfectly well. For a better quantitative reliability however, a more careful treatment of the medium correction procedure is needed.

3. Results

In figs. 1–4 we represent some outputs corresponding to various physical situations considered in refs. [6,7]. The computations are done on an IBM 360 with an IBM 1627-II drum-plotter online, and in standard FORTRAN IV.

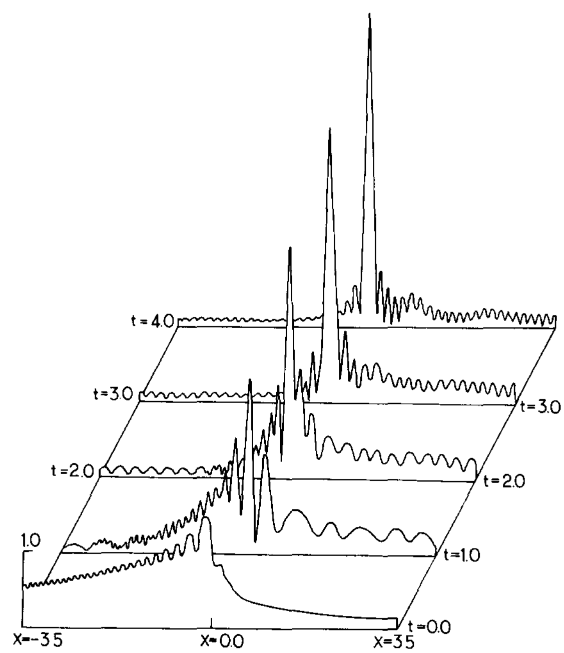

Fig. 1. Development and collapse of a soliton-like structure in the electric field for $p = 1$ and in one spatial dimension. The collapse process consists in ever increasing height of the peak with simultaneous decrease in spatial extent of the soliton. The initial field used was the stationary solution ($\partial_t A = 0$) whose stability is under question.

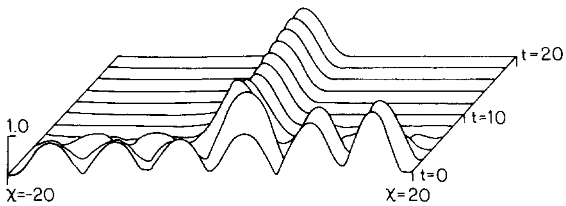

Fig. 2. Same as fig. 1, but for different input and integration parameters. The input for A was a displaced exponential: $\exp(iax)+b$ multiplied by a damping function. Development of a central quasi-stable almost stationary soliton is observed.

In fig. 1, occurrence of the modulational instabilities in the stationary solution ($\partial_t A = 0$) with development and collapse of a soliton structure in 1 + 1 dimension is depicted. The stationary solution used as the input is obtained by solving the (complex) second Painlevé equation:

$$\partial_x^2 A(x) = (x - p|A|^2)A = 1, \tag{3.1}$$

with the help of the DE package [12]. In the region $x \gg 0$, where a blow-up of the numerical solution is possible, an extrapolation to the asymptotic solution $-\pi(G_i + A_i)$ is used, where $G_i(x)$ and $A_i(x)$ represent the Airy functions [13]. We put 512 points across the grid and used 40 time steps. The execution took 18 min of elapsed time (plotting included), with approximately 7 min used for the initialization by the DE package.

In fig. 2, a spatiotemporal emission and development of a slowly growing soliton-like perturbation in 1 + 1 dimension is presented. Additional collapsing structure is seen outside the displayed interval. The stability of the soliton here is enhanced by the smoothing procedure which introduces a local damping, and whose effect is more pronounced when there are fewer points across the grid. Numerical procedure is the same as in the previous example, only the initial field and various integration parameters are different. This time only 128 points are used, and 200 time steps. The elapsed time amounted to 9 min.

Figs. 3 and 4 are obtained by integration of the system of equations (2.11) in 2 + 1 dimensions, with A taken along the x-axis. The initial field A_0 is chosen as a hyperbolic secant in the x-direction, while the initial density $N_0 = -|A_0|^2$ is modulated to induce a collapse process. The collapse process consists in unbounded localization of the electric field inside a density cavity of ever increasing depth and decreasing spatial extent. The value of ky varied from $-\pi/2$ to $\pi/2$ over the whole of the y-interval. Fig. 3 represents a two-dimensional in-

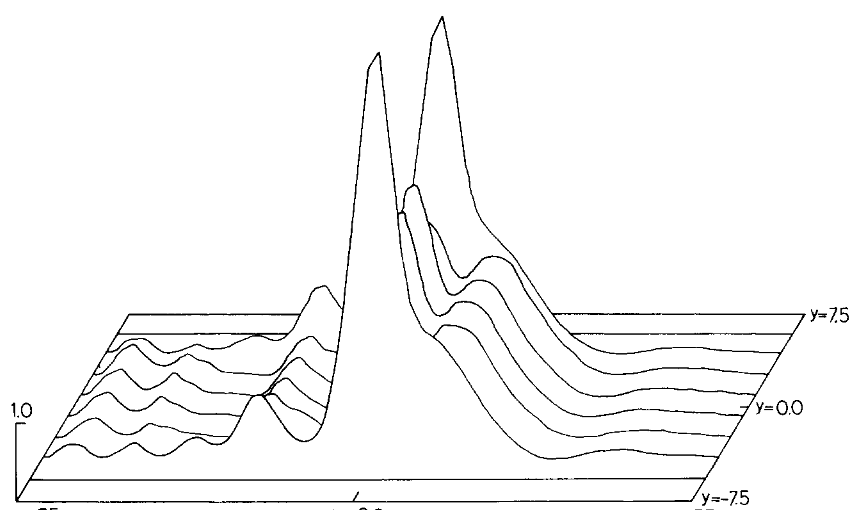

Fig. 3. Profile of the electric field intensity in two spatial dimensions for $p = 1$ at $t = 1.5$, eqs. (2.11), with two collapsing peaks. The input was $\hat{x}$ sech(x) times a damper.

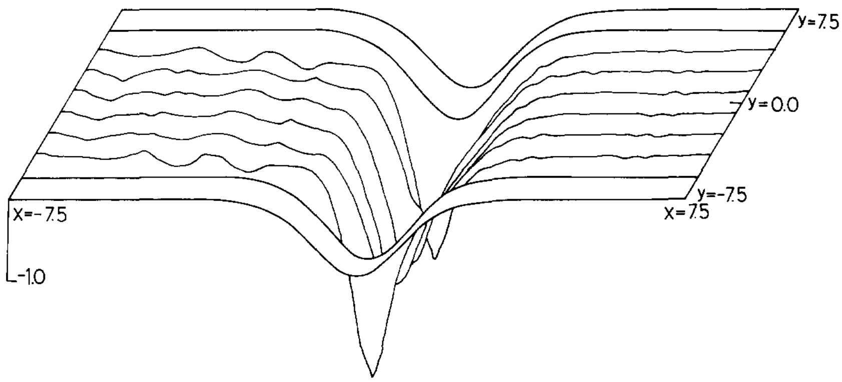

Fig. 4. The density profile corresponding to fig. 3. Value of the damping coefficient in eq. (2.11b) was $\gamma = 10$. The input for N was $-(1+\cos ky)\mathrm{sech}^2 x$, with ky varying approximately from $-\pi/2$ to $\pi/2$ over the whole of the y-interval.

tensity distribution at $t = 1.5$ and fig. 4 the corresponding density profile. It is seen that deep density cavities coincide with the peaks of the electric field. Taking of these profiles on a 64-by-64 grid, including the plotting on four intermediate time points took 35 min of elapsed time.

References

[1] V.L. Ginzburg, The Propagation of Electromagnetic Waves in Plasmas (Pergamon, New York, 1970) 2nd. ed.
[2] V.E. Zakharov, Sov. Phys. JETP 35 (1972) 908.
V.E. Zakharov and M. Rubenchik, Sov. Phys. -JETP 38 (1974) 494.
[3] G.J. Morales and Y.C. Lee, Phys. Rev. Lett. 33 (1974) 1016; Phys. Fluids 20 (1977) 1135.
[4] K. Elsässer and H. Schamel, Plasma Phys. 19 (1977) 1055.
H. Schamel and K. Elsässer, Plasma Phys. 20 (1978) 837.
[5] V.B. Gil'denburg and G.M. Fraiman, Sov. Phys. -JETP 42 (1975) 816.
[6] J.C. Adam, A. Gourdin Serveniere and G. Laval, Phys. Fluids 25 (1982) 376.
[7] N.R. Pereira, R.N. Sudan and J. Denavit, Phys. Fluids 20 (1977) 936.
N.R. Pereira and G.J. Morales, Phys. Fluids 24 (1981) 1812.
[8] J.P. Armstrong, Phys. Fluids 10 (1967) 1269.
S.A. Orszag, J. Fluid Mech. 49 (1971) 75; Stud. Appl. Math. 50 (1971) 293.
Y. Salu and G. Knorr, J. Comput. Phys. 17 (1975) 68.
H. Schamel and K. Elsässer, J. Comput. Phys. 22 (1976) 501.
Y.S. Sigov and Y.V. Khodirev, Dokl. A.N. SSSR 229 (1976) 833.
[9] E.A. Sziklas and A.E. Siegman, Appl. Opt. 14 (1975) 1874.
[10] M. Lax, J.H. Batteh and G.P. Agrawal, J. Appl. Phys. 52 (1981) 109.
[11] M. Lax, G.P. Agrawal, M.R. Belić, B.J. Coffey and W.H. Louisell, to be published.
M.R. Belić, PhD thesis, City University of New York (1980) unpublished, chap. 2.
J.V. Moloney, M.R. Belić and H.M. Gibbs, Opt. Commun. 41 (1982) 379.
[12] L.F. Shampine and M.K. Gordon, Computer Solution of Ordinary Differential Equations (W.H. Freeman, San Francisco, 1974).
[13] Handbook of Mathematical Functions, eds. M. Abramowitz and I.A. Stegun (Dover, New York, 1970) p. 446.